Dynamically biased statistical model for the ortho/para conversion in the H2+H3+ → H3++ H2 reaction

Susana Gómez-Carrasco, Lola González-Sánchez, Alfredo Aguado, Cristina Sanz-Sanz, Alexandre Zanchet et al.

Additional information on J. Chem. Phys.

Dynamically biased statistical model for the ortho/para conversion in the $H_2 + H_3^+ \rightarrow H_3^+ + H_2$ reaction

Susana Gómez-Carrasco,[1] Lola González-Sánchez,[1] Alfredo Aguado,[2] Cristina Sanz-Sanz,[3] Alexandre Zanchet,[3] and Octavio Roncero[3,a)]
[1]*Departamento de Química Física, Facultad de Ciencias Químicas, Universidad de Salamanca, 37008 Salamanca, Spain*
[2]*Unidad Asociada UAM-CSIC, Departamento de Química Física, Facultad de Ciencias C-XIV, Universidad Autónoma de Madrid, 28049 Madrid, Spain*
[3]*Unidad Asociada UAM-CSIC, Instituto de Física Fundamental (IFF-CSIC), C.S.I.C., Serrano 123, 28006 Madrid, Spain*
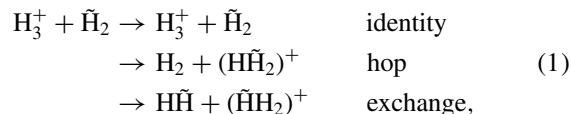
In this work we present a dynamically biased statistical model to describe the evolution of the title reaction from statistical to a more direct mechanism, using quasi-classical trajectories (QCT). The method is based on the one previously proposed by Park and Light [J. Chem. Phys. **126**, 044305 (2007)]. A recent global potential energy surface is used here to calculate the capture probabilities, instead of the long-range ion-induced dipole interactions. The dynamical constraints are introduced by considering a scrambling matrix which depends on energy and determine the probability of the identity/hop/exchange mechanisms. These probabilities are calculated using QCT. It is found that the high zero-point energy of the fragments is transferred to the rest of the degrees of freedom, what shortens the lifetime of H_5^+ complexes and, as a consequence, the exchange mechanism is produced with lower proportion. The zero-point energy (ZPE) is not properly described in quasi-classical trajectory calculations and an approximation is done in which the initial ZPE of the reactants is reduced in QCT calculations to obtain a new ZPE-biased scrambling matrix. This reduction of the ZPE is explained by the need of correcting the pure classical level number of the H_5^+ complex, as done in classical simulations of unimolecular processes and to get equivalent quantum and classical rate constants using Rice–Ramsperger–Kassel–Marcus theory. This matrix allows to obtain a ratio of hop/exchange mechanisms, $\alpha(T)$, in rather good agreement with recent experimental results by Crabtree *et al.* [J. Chem. Phys. **134**, 194311 (2011)] at room temperature. At lower temperatures, however, the present simulations predict too high ratios because the biased scrambling matrix is not statistical enough. This demonstrates the importance of applying quantum methods to simulate this reaction at the low temperatures of astrophysical interest. © *2012 American Institute of Physics*. [http://dx.doi.org/10.1063/1.4747548]

I. INTRODUCTION

H_3^+ is the most abundant molecular ion in space and is considered to be the universal protonator.[1–4] Models to estimate the concentration of this cation, and its isotopomers, are used to follow the dynamics of ionospheres of outer planets as a function of solar fluence[5–7] and in isotopic exchange processes in low pressure plasmas of H_2/D_2 mixtures.[8,9] H_3^+ is formed in the $H_2 + H_2^+ \rightarrow H_3^+ + H$ reaction, and its deuterated variants via the subsequent $HD + H_3^+ \rightarrow H_2D^+ + H_2$ proton-deuteron exchange reaction, and isotopic variants. These last reactions, widely studied experimentally,[10–17] are considered to be responsible for the high relative abundance of deuterated species, $\approx 10^4$ times higher than the D/H ratio of the galaxy,[18–21] attributed to zero-point energy differences important at the low temperatures of the interstellar medium.[14,22] It has been found that the deuterated fraction can be used as a tracer of massive star formation.[21] Of par-

ticular interest is the spin-statistics of these species, which determines selection rules for the ortho/para conversion of H_3^+.[12,16,23–27]

The most detailed theoretical studies performed until now are based on the statistical approach, including nuclear spin symmetry constraints.[16,17,28] The applicability of these methods relies on the formation of long-lived H_5^+ complexes, in which a complete randomization of energy among all degrees of freedom is produced. In such situation 3 different channels can be distinguished:

$$
\begin{aligned}
H_3^+ + \tilde{H}_2 &\rightarrow H_3^+ + \tilde{H}_2 & \text{identity} \\
&\rightarrow H_2 + (H\tilde{H}_2)^+ & \text{hop} \\
&\rightarrow H\tilde{H} + (\tilde{H}H_2)^+ & \text{exchange,}
\end{aligned} \quad (1)
$$

which statistical weights are 1/10, 3/10, and 6/10, respectively. This statistical behavior is expected to be valid only at relatively low collision energy, because the well of the H_5^+ complex is rather shallow, of ≈ 3044 cm^{-1}.[29,30] In fact, several statistical models were built giving different weights to the exchange mechanism,[16,17,28] assuming the existence or

a)Author to whom correspondence should be addressed. Electronic mail: octavio.roncero@csic.es.

not of a scrambling process, which would allow the exchange of any of the hydrogen atoms within the complex. It is therefore important to perform dynamical calculations on this reaction to provide information about the relative importance of each of the three possible mechanisms of Eq. (1).

Dynamical calculations require global potential energy surfaces (PESs). In the last years several PES's, of increasing accuracy, have appeared in the literature.[29–35] The exchange reaction barrier is rather low, below the zero-point energy, so that all identical nuclei can permute, subject to the symmetry constraints imposed by nuclear spin angular momenta,[23,24,26] as experimentally confirmed by measurements in plasmas at 300–500 K.[12,13] All this makes extremely difficult to perform complete quantum calculations including the 12 degrees of freedom (9 vibrational and 3 rotational), considering the whole permutation group of symmetry. For this aim, proper coordinates should be designed, as the democratic hyperspherical coordinates developed recently by Kuppermann.[36] The use of these coordinates requires the evaluation of the hyperspherical harmonics, a work still in progress.[37,38]

One of the first simulations of the title reaction was the quasi-classical study performed by Moyano and Collins,[34] who found discrepancies with the available experimental results, which were attributed to possible quantum effects and to the accuracy of the PES. Recently seven-degree-of-freedom quantum scattering calculations of the $H_2 + H_2D^+$ reaction have been reported,[39] for state-selected initial states, which do not take into account the permutation symmetry. This reduced dimensionality model uses reactants Jacobi coordinates, which does not distinguish among the different rearrangement channels.

The aim of this work is to combine statistical methods, which account for the nuclear spin selection rules, and dynamical methods, based on quasi-classical trajectories (QCT) in this case, to properly account for the hop/exchange ratios. For that purpose we shall follow the treatment of Park and Light in Ref. 28, introducing the dynamical results in the so-called scrambling probability, S^M, as a dynamical bias, possibility already mentioned in Ref. 28. Moreover, until now most statistical models have only used asymptotic expansions of the potential in which H_3^+ is treated as a point charge interacting with a H_2 molecule, including its induced electric dipole and quadrupole. Here, we shall use a global PES recently proposed which describes very satisfactorily the long-range interactions, going beyond the point charge model for H_3^+ using a triatomics-in-molecules (TRIM) treatment.[29]

The organization of the paper is as follows. In Sec. II A the statistical method of Park and Light[28] is outlined to introduce the notation. Section II B describes the procedure followed here to calculate the capture probabilities. Section II C shows the details of QCT calculations and in Sec. II D how these results are used to obtain the scrambling probability, S^M. Section II E describes the zero-point energy (ZPE) effect on the dynamics by only considering a fraction of the ZPE of the reactants. Finally, Sec. II F describes the rate constants, making emphasis in the ortho/para rates and hop/exchange ratio, and some conclusions are extracted in Sec. III.

II. THEORETICAL METHODOLOGY

A. Statistical model

In this work we closely follow the statistical treatment of Park and Light,[28] in the version of the separate proton-scrambling mechanism. We simply outline the method to explain the differences introduced here to bias the scrambling probability by dynamical calculations.

The state-to-state canonical reaction rate coefficient is given by[28]

$$K_{sr,M's'r'}(T) = \frac{h^2}{[j_d][j_t][I_2][I_3]} \left(\frac{1}{2\pi \mu k_B T} \right)^{3/2}$$
$$\times \int dE \; e^{-(E-E_{sr})/k_B T} \; N_{sr,M's'r'}(E), \quad (2)$$

with $[J] = 2J + 1$ and where $s \equiv (I_2, I_3)$ and $r \equiv (j_d, j_t, \omega_t)$ denote the nuclear spin and rotational state of H_2 and H_3^+, respectively, in each rearrangement channel M. M is 1 for the initial state (or identity channel, and is omitted for reactants for simplicity), 2 for the hop mechanism, and 3 for the exchange mechanism. k_B is the Boltzmann constant, and E_{sr} is the sum of the energy of the initial states of H_2 and H_3^+ reactants. The H_3^+ energy levels and quantum numbers used in this work are listed in Table I. The triatomic bound states were calculated with the PES of Ref. 29 in hyperspherical coordinates to properly assign the symmetry using an iterative Lanczos method, as described elsewhere.[40,41]

The state-to-state cumulative reaction probabilities (CRPs), $N_{sr,M's'r'}(E)$, are given by

$$N_{sr,M's'r'}(E) = \sum_{JI} [J][I] P_{sr,M's'r'}^{JI}(E), \quad (3)$$

where J, I are quantum numbers associated to the total orbital angular momentum and total nuclear spin, respectively. In this work we shall use a body-fixed description, which is essentially equivalent to the space-fixed treatment of Park and Light.[28] In the centrifugal sudden (CS) approximation used, the helicity quantum number Ω is conserved and equal to the

TABLE I. Rotational levels of H_3^+ calculated with hyperspherical coordinates using the PES of Ref. 29. All the levels correspond to the ground $(0, 0^0)$ vibrational state (with energy 4359.52 cm^{-1} for the non-physical state of $j_t = 0$, taken as zero of energy), but different rotational states j_t, ω_t, and irreducible representation, Γ, of the permutation-inversion group, isomorphic with the D_{3h} group. The nuclear spin, I_3, is also indicated for ortho ($I_3 = 3/2$) and para ($I_3 = 1/2$) states.

j_t	ω_t	Γ	I_3	Energy (cm^{-1})
1	1	E''	1/2	64.04
1	0	A_2'	3/2	86.86
2	2	E'	1/2	169.10
2	1	E''	1/2	237.07
3	3	A_2''	3/2	314.97
3	2	E'	1/2	427.50
3	1	E''	1/2	494.17
3	0	A_2'	3/2	516.26

sum of the helicities of the fragments in the total body-fixed frame, ν and Ω_t for H_2 and H_3^+ fragments, respectively.

The state-to-state reaction probabilities, $P_{sr,M's'r'}^{JI\Omega}(E)$, are the sum of the square of the collision S-matrix over the projections ν and Ω_t, such that $\Omega = \nu + \Omega_t$ is conserved. It should be noted, that in this CS approach, Ω becomes a good quantum number. Following the separate proton-scrambling statistical approach of Park and Light,[28] these probabilities $P_{sr,M's'r'}^{JI\Omega}(E)$ are given by

$$
P_{sr,M's'r'}^{JI\Omega}(E) = \sum_{\nu\Omega_t} \sum_{\nu'\Omega_t'} \Bigg\{ \left[1 - W_{sr\nu\Omega_t}^{J\Omega}(E) \right] \delta_{sr\nu\Omega_t, s'r'\nu'\Omega_t'} \delta_{M'1}
$$

$$
+ g_{Is} \gamma_{sIs'}^{M'} W_{sr\nu\Omega_t}^{J\Omega}(E)\, W_{s'r'\nu'\Omega_t'}^{J\Omega}(E) \Bigg/
$$

$$
\sum_{M''s''r''\nu''\Omega_t''} \gamma_{sIs''}^{M''} W_{s''r''\nu''\Omega_t''}^{J\Omega}(E) \Bigg\}, \qquad (4)
$$

where $W_{s'r'\nu'\Omega_t'}^{J\Omega}(E)$ are the capture probabilities defined below. g_{Is} is an element of the nuclear spin statistical weight (NSSW) matrix[28]

$$
g = \begin{Bmatrix} 2 & 0 & 2 & 2 \\ 0 & 4 & 4 & 4 \\ 0 & 0 & 0 & 6 \end{Bmatrix}, \qquad (5)
$$

indicating how many functions of total spin I can be formed with spin fragments functions $s = (I_2, I_3)$, and ordered as $s = (0, 1/2), (0, 3/2), (1, 1/2), (1, 3/2)$, and $I = 1/2, 3/2, 5/2$.

In Eq. (4), the spin branching ratio matrices, $\gamma_{sIs'}^{M'}$, for each mechanism M' are given by

$$
\gamma_{sIs'}^{M'} = (2I + 1) S_{M'} \Gamma_{sIs'}^{M'} \big/ e_s e_{s'}, \qquad (6)
$$

with $e_s = 1$ or 2 for $I_3 = 3/2$ or $1/2$, respectively. This factor is introduced to consider that I_3 spin functions belong to the E representation of the S_3 permutation group, and to form a total function of A_2 symmetry has to be combined with r rovibrational functions of E symmetry, so that the direct product gives $E \times E = A_1 + A_2 + E$. Among these last functions only those of A_2 symmetry exist, and this fact is accounted for by the factor e_s.

$S_{M'}$ in Eq. (6) is the scrambling probability,[28] which corresponds to the number of channels for each mechanism, i.e., 1/10, 3/10, and 6/10 for identity ($M' = 1$), hop ($M' = 2$) and exchange ($M' = 3$) mechanisms, respectively. These values correspond to the high temperature statistical limit for reasons which will be discussed below. The dynamical constraints are introduced by varying this matrix as also described below.

The spin modification matrix $\Gamma_{sIs'}^{M'}$[28] in Eq. (6) is given by

$$
\Gamma_{sIs'}^{M'} = \sum_{i_2 i_2'} |\langle I, I_z, I_3, i_2, I_2 | \mathcal{O}_{M'} | I, I_z, I_3', i_2', I_3' \rangle|^2, \quad (7)
$$

with $\mathcal{O}_{M'} = E, p_{ad} p_{be}$ or p_{cd} for $M' = 1, 2$, or 3, respectively, where $p_{\alpha\beta}$ is the permutation operator. Those elements are tabulated in Table II of Ref. 28.

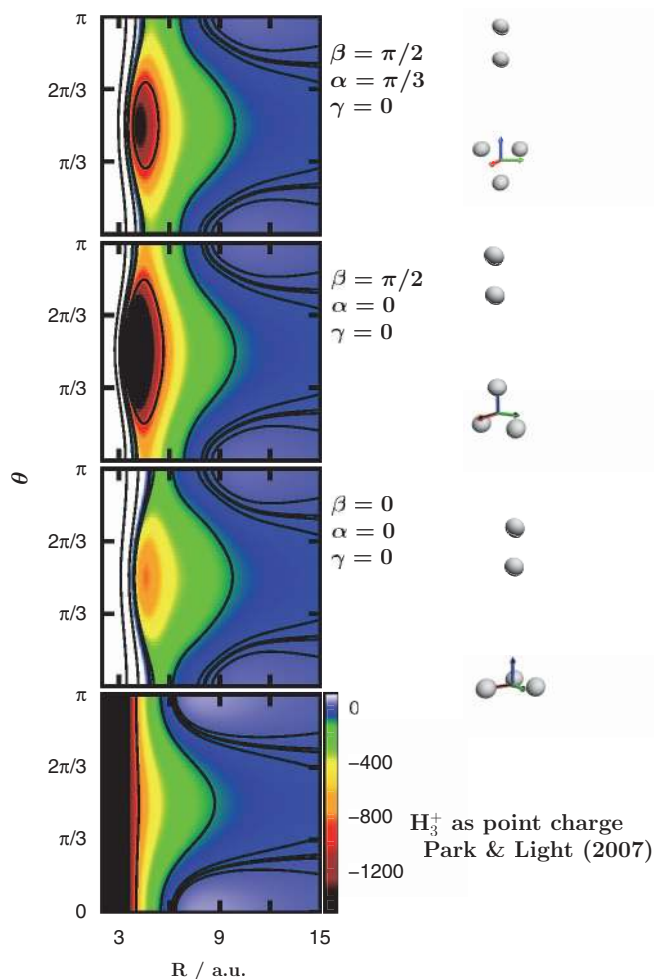FIG. 1. Asymptotic $H_3^+ + H_2$ potential energy surface (in cm^{-1}) as a function of the center-of-mass separation, R, and the angle θ between $\mathbf{R}$ and $\mathbf{r}$, the H_2 internuclear vector. The lower panel corresponds to the asymptotic potential of Ref. 28 which describes H_3^+ as a point charge. The three upper panels correspond to three different orientations of the H_3^+ subunit, described by the Euler angles (α, β, γ) described in the text, using the global potential of Ref. 29. In this plot H_2 and H_3 are frozen in their asymptotic equilibrium geometries.

B. Capture probability

In Ref. 28, the interaction potential was approximated by the long-range interaction between a point charge, representing H_3^+, and the induced electric dipole and quadrupole of H_2, and it is shown in the bottom panel of Fig. 1. Such potential interaction goes to $-\infty$ for short distances and does not take into account charge distribution and shape of H_3^+. In this work we consider the full potential energy surface developed in Ref. 29, which describes correctly the asymptotic behavior for long distances and also the potential well, as it is shown in Fig. 1. In what follows, this PES will be used to calculate the capture probabilities, freezing the H_2 and H_3^+ at their equilibrium distances, since only the ground vibrational levels of the two monomers can be populated at the energies of interest here.

In order to calculate the potential matrix elements, it is convenient to use a body-fixed frame, defined such as the z-axis is parallel to $\mathbf{R}$, the vector joining the H_2 and H_3^+

center-of-masses, and the H_2 molecule internuclear vector, **r**, is in the xz body-fixed frame. The body-fixed basis set angular functions considered are defined as

$$\mathcal{Y}_{\Omega r \equiv j_d, j_t, \omega_t}^{J m_J} = \sqrt{\frac{2J+1}{8\pi^2}} \, D_{m_J \Omega}^{J*}(\phi_R, \theta_R, \phi_r)$$

$$\times \sqrt{\frac{2j_t+1}{8\pi^2}} \, D_{\Omega_t \omega_t}^{j_t*}(\alpha, \beta, \gamma) \, \mathcal{P}_{j_d \nu}(\theta) \quad (8)$$

with $\Omega = \Omega_t + \nu$, and $\mathcal{P}_{j_d \nu}$ being normalized associated Legendre functions. $(\phi_R, \theta_R, \phi_r)$ are the Euler angles connecting the body-fixed and space-fixed frames. H_3^+ frozen at its triangular equilibrium geometry is described by the symmetric top eigen-functions,[42] $D_{\Omega_t \omega_t}^{j_t*}(\alpha, \beta, \gamma)$. The (α, β, γ) Euler angles describe the orientation of the principal axes system of H_3^+ (with z' perpendicular to the plane of the molecule) and the body-fixed frame described above (with z parallel to **R**). Finally, θ is the angle between **r** and **R**. The potential depends directly on $\alpha, \beta, \gamma, \theta$ angles, so that its matrix elements, $\langle \mathcal{Y}_{\Omega r}^{J m_J} | V | \mathcal{Y}_{\Omega r'}^{J m_J} \rangle$, are calculated numerically by representing these functions in grids. Polar angles, such as β and θ are described by Gauss-Legendre quadrature points while azimuthal angles, α and γ, by equidistant points. This is accomplished here by using 40 quadrature points for each angle.

Similarly to what was done in Ref. 28, here we only consider diagonal potential matrix elements in the body-fixed frame, i.e., $\Omega = \Omega'$ and $r = r'$, and the Coriolis couplings among different Ω values are neglected. Thus Ω becomes a good quantum number and is used in the place of the parity Π in the sums involved for the CRP of Eq. (3). For each collection of quantum numbers (J, Ω, r), or channel, an effective potential can be defined as

$$V_{eff}^{(J,\Omega,r)}(R)$$

$$= \langle \mathcal{Y}_{\Omega r}^{J m_J} | V | \mathcal{Y}_{\Omega r}^{J m_J} \rangle$$

$$+ \frac{J(J+1) + j_d(j_d+1) + j_t(j_t+1) - 2\Omega^2 + 2\nu\Omega_t}{2\mu R^2}$$

$$+ E_{j_d} + E_{j_t \omega_t}, \quad (9)$$

where E_{j_d} and $E_{j_t \omega_t}$ are the energies of the isolated diatomic and triatomic fragments, respectively. The well depth of the effective potential depends on the initial states of H_3^+ and H_2. For $J > 0$, the addition of the rotational barrier diminishes the depth of the effective well describing the H_5^+ complex, and for moderately high J, ≈ 20, the well nearly disappears. This effect is not present in the point charge asymptotic model potential used by Park and Light,[28] in which the potential tends to $-\infty$ as $R \to 0$. Also, in that model the effective potential only depends on the orientation of the H_2 molecule, and not on that of H_3^+ and its rotational level.

The capture probabilities are calculated as in the simplest model of Ref. 28

$$W_{srv\Omega_t}^{J\Omega}(E) = \begin{cases} 0 & E < V_{max} \\ 1 & E > V_{max} \end{cases}, \quad (10)$$

i.e., the system is trapped for energies above the rotational barrier, V_{max}, provided that the effective potential presents a well.
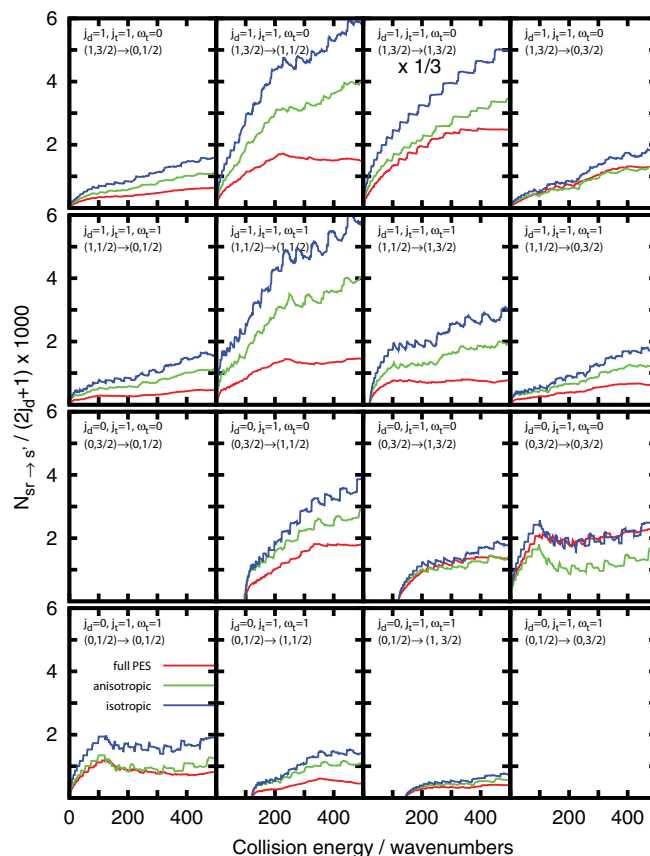

FIG. 2. Cumulative reaction probabilities sum, $N_{sr,s'}(E) = \sum_{M'r'} N_{sr,M's'r'}(E)$ (divided by $(2j_d + 1) \times 1000$) for the 2 first states of H_2 and H_3 (para and ortho for the ground and first excited). The initial state and final nuclear spin are marked as $(I_2, I_3) \to (I_2', I_3')$ in each panel. Three different potentials are considered: the isotropic and anisotropic asymptotic potentials used by Park and Light[28] in which H_3^+ is considered as a point charge, and the full PES of Ref. 29.

In Fig. 2 we present the CRPs obtained for some initial states (summed over final rotational states and rearrangement channels) using three models of potential interaction: the asymptotic model, in which H_3^+ is a point charge, in the isotropic and anisotropic models used by Park and Light,[28] and the full potential of Ref. 29. As the anisotropy of the PES increases the CRP gets lower, simply because more angular configurations become inaccessible, disrupting the approach of the two reagents. These effects get magnified as the rotational excitation of either H_2 and H_3^+ increases, and are very sensitive to the stereodynamics, since the preferred direction of attack corresponds to the H_2 center-of-mass in the plane of H_3^+. In general, for the non-diagonal terms, the full PES model always yields to lower probabilities simply because the capture probability of the initial states get lower, as a consequence of the larger anisotropy. The diagonal $(I_2, I_3) \to (I_2, I_3)$ terms contain the elastic (which should always be larger for the full PES model), inelastic and reactive probabilities, and for this reason they do not show a clear trend.

C. Quasi-classical trajectory calculations

The reaction dynamics of the title reaction is studied using quasi-classical trajectories, using an Adams-Bashforth-Moulton predictor-corrector integrator of variable step in

Cartesian coordinates. The initial conditions are determined using a generalization of the Monte Carlo sampling method introduced by Karplus *et al.*[43] for atom-diatom reactions, as explained below.

The vibrational energy is obtained as that of the ground state of the fragment for j_d or j_t equal to zero, while the rotational energy is obtained by subtracting the vibrational contribution to the exact eigenvalue obtained for the desired rotational state. For both fragments, H_2 and H_3^+, the internal coordinates are obtained from classical turning points randomly selected. For H_2 the two classical turning points of the ground vibrational level are obtained following a standard Newton-Raphson procedure. For H_3^+, this is done in two steps: first, the two internal hyperspherical angles are selected randomly using isotropic distributions and, second, the two classical turning points are searched on the monodimensional potential as a function of the hyperradius, as in the diatomic case. Once the internal coordinates are obtained, the orientation of the two fragments is obtained by a random selection over the corresponding Euler angles, assuming isotropic angular probability distributions. Finally, H_3^+ center-of-mass is set at the origin of coordinates, while H_2 center-of-mass is set at a distance of $R = 14$ Å . The impact parameter is randomly selected in the interval $[0, b_{max}]$, according to a quadratic distribution, so that $R_x = b \cos \phi$, $R_y = b \sin \phi$, $R_z = \sqrt{R^2 - b^2} + \delta v_r \tau$. Here ϕ is a random number in an isotropic distribution between 0 and 2π. v_r is the relative velocity between the two reactants, τ is the sum of the vibrational period of the two fragments and δ a random number between 0 and 1. This last factor shifts the initial distance between the two reactants by a random factor and is introduced to warranty that the relative vibrational phase of the two reactants at the moment of the collision is random.

The initial velocities correspond to the sum of rotational and translational ones. The translational energy is divided between the two center-of-mass in opposite direction so that the total linear momentum is zero. The initial rotational energy of the diatomic fragment is completely determined by the rotational quantum number j_d.[43] The $\mathbf{j}_d$ vector is set to be in the plane perpendicular to the H_2 internuclear vector, $\mathbf{r}$, and determined by one random number isotropically distributed between 0 and 2π. For H_3^+, the z-component of $\mathbf{j}_t$, ω_t, is fixed, and the other two components of the angular velocity vector $\vec{\omega}$ are optimized to fit the rotational energy

$$E_{rot} = E^J - E^{J=0} = \frac{1}{2} \vec{\omega} \ \mathbf{I} \ \vec{\omega}. \qquad (11)$$

In this expression, the inertia tensor $\mathbf{I}$ is obtained from the internal coordinates previously obtained in the triatomic body-fixed frame. The rovibrational eigenvalues, E^J, are obtained numerically for the $(0, 0^0)$ vibrational state using hyperspherical coordinates.[40,41] With this procedure, the fitted initial rotational energy has an error lower than 10^{-3} cm^{-1}, ω_t is exact, but the triatomic angular momentum j_t is only approximate and, in general, not integer.

The impact parameter runs from 13 Å for the lowest energy considered, 8 cm^{-1}, to 6 Å for the highest one of 800 cm^{-1}. Finally, the trajectories are stopped when the velocity between the two fragments is positive and their dis-

tance larger than 16 Å. The collision time is defined as the average of the time required in each trajectory to reach thus distance.

The potential energy used is the full dimensional PES of Ref. 29. This potential is described using a triatomic-in-molecules formalism, which allows to describe correctly the long range dependence of the H_3^+ ion with the induced dipole and quadrupole of H_2, as shown in Fig. 1. To improve the accuracy of the TRIM model at short distances, two analytical five-body terms are added. The derivatives of this potential are calculated in internal coordinates using a mixed numerical/analytical method: the TRIM derivatives are obtained numerically, while the five-body terms are analytical. The energy thus obtained along the integrated trajectories is conserved with an error lower than 10^{-2}cm^{-1}. These trajectories correspond to complex dynamics with the formation of the long-lived H_5^+. Trajectories with larger errors were neglected. The conservation of total angular momentum was not analyzed, and back propagation was not done because of the high computational effort required. The average propagation times are between 10 and 20 min of CPU per trajectory. Due to the large computational cost the calculations have been performed in GRID computing, using the IBERGRID facilities.

The initial ZPE is rather high, ≈ 6538 cm^{-1},[44] compared to the initial collision energies considered, <1000 cm^{-1}. The initial ZPE of the reactants is set in the initial conditions. Along the collision dynamics the ZPE can be distributed among all the degrees of freedom due to the classical character of the dynamical calculations. This makes that the final internal energy is not properly quantified, and energies much lower than the allowed ZPE are obtained. One may think that one possible way to solve this problem is by Gaussian binning methods.[45,46] This procedure has been applied recently to the study of the triatomic $D^+ + H_2$ and $H^+ + D_2$ reactions providing a very good agreement with experiments.[47] However, in the present five-atom case the ZPE is very high. This implies a very wide energy range of internal energy of the two products. Most of the trajectories would end having internal energies very different from the real ones, having a negligible contribution. This problem would then require to increase by many orders of magnitude the number of trajectories required to get converged results. This makes impractical the use of such method to correct the ZPE of products in H_5^+ due to the long propagation times. Here another simple method to solve the ZPE problem will be used as described below in Sec. II E.

In this work we will only focus on the final distribution of products between the different rearrangement channels. The ratio between the three different channels shown in Eq. (1) are obtained with QCT calculations. Of particular relevance is the factor $\alpha(T) = K^{hop}/K^{exchange}$ between the hop and exchange mechanism.[13,17] Here, we first evaluate this factor as a function of energy as $\alpha(E) = P^{hop}/P^{exchange}$, where P^M are the QCT probabilities. These probabilities are calculated including all trajectories with an impact parameter lower than b_{max} for a fixed collisional energy. This b_{max} corresponds to the largest value of the impact parameter for which hop or exchange probability are non-zero. We have found that these quantities converge rapidly with the number of trajectories.
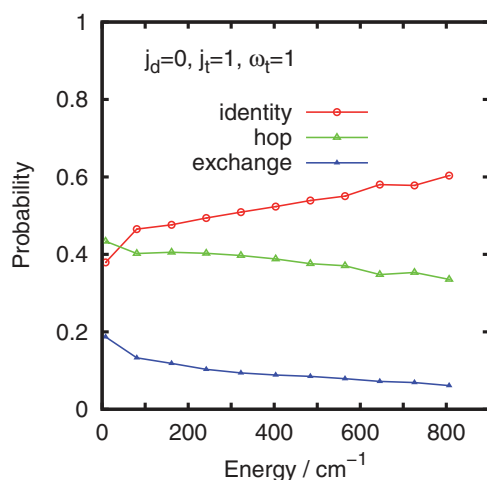
FIG. 3. Probabilities for ending in the three rearrangement channels (identity, hop, and exchange) determined with QCT calculations, for initial $H_3^+(j_t = 1, \omega_t = 1)$ and $H_2(j_d = 0)$ reactants. The results for other triatomic ($j_t = 2, 3$) and diatomic ($j_d = 1$) states provide essentially the same results.

For this purpose in this work we use 12 000 trajectories calculated for each collisional energy and each initial state of the fragments. The collisional energies calculated are 8, 80, 160,…, 800, 1200, and 3200 cm^{-1}, for $j_d = 0$ and 1, and for the 8 rotational states of H_3^+ listed in Table I, corresponding to $j_t = 1, 2,$ and 3.

The probabilities for ending in each of the three rearrangement channels are shown in Fig. 3 for the case of the ground rotational states of the reactants. For all the rest of the cases examined the probabilities obtained are very similar. Typically, at low energies, $E = 8$ cm^{-1}, the identity and hop channels are both nearly 40%, and the remaining 20% corresponds to the exchange mechanism. As energy increases, the hop and exchange probabilities decrease, while that of the identity channel increases up to a value of 75%. The same behavior is observed as the initial excitation of H_3^+ increases, even when the rotational energy increases from 64 up to 515 cm^{-1}. The change between $j_d = 0$ and 1 of H_2 is slightly more important, but still pretty small. The rotational and translational energies are small fractions of the ZPE of the system (≈ 6538 cm^{-1}). In the interaction region, the large ZPE energy can be distributed rather freely among the different degrees of freedom. The variation of the probabilities with collision energy in Fig. 3 should thus correspond to the dynamics in the entrance channel, just before the ZPE energy may flow among the different degrees of freedom.

To interpret these results the identity/hop/exchange probabilities and the collision time are displayed in the left panels of Fig. 4 as a function of the impact parameter, b, for $H_3^+(j_t = 1, \omega_t = 1) + H_2(j_d = 0)$ at three different collision energies. The collision time for $b < 13$ Å does not depend on the impact parameter and shows the expected increase with the decreasing of the translational energy. However, for high impact parameters, $b > 13$ Å, the two lower energies show a rather significant increase on the collision time. At 800 cm^{-1} the trajectories are not deviated by the potential and no rearrangement is produced. At the same time, for the higher b-values the identity probability increases very fast, while the
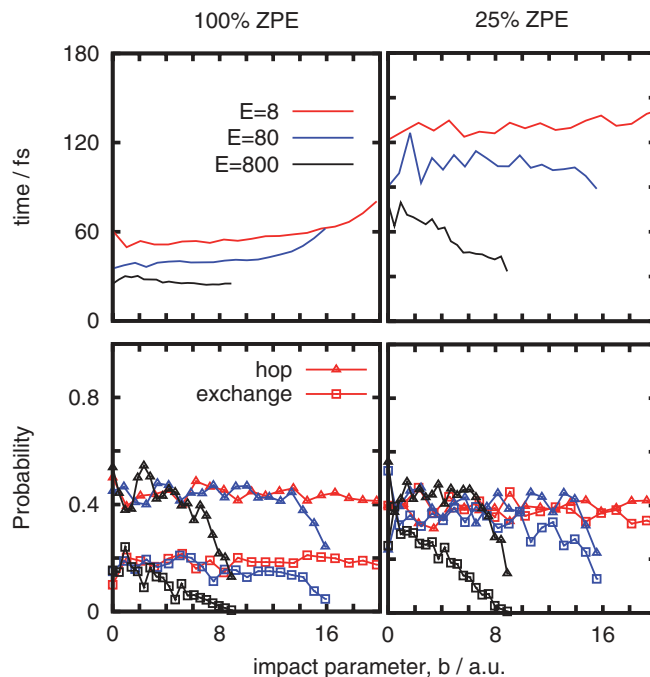

FIG. 4. Hop and exchange probabilities (bottom panels), described by full triangle and empty square symbols, respectively, and collision time (top panel) versus the impact parameters for $H_3^+(j_t = 1, \omega_t = 1) + H_2(j_d = 0)$ collisions at translational energies of 8, 80, and 800 cm^{-1} (described by red, blue, and black lines, respectively). Left/right panels show the QCT results considering initial all/25% of the true zero-point energy.

hop and exchange ones decrease. It is important to note, however, that the hop/exchange ratio remains nearly the same as a function of b below 13 Å, while for higher b's the hop probability decreases faster than the exchange one. This behavior produces an increase of the hop/exchange ratio, α, as a function of the collision energy, as displayed in Fig. 5. This is simply because the impact parameter decreases with increasing collision energy, up to a plateau which is near 6 Å at $E \approx 700$ cm^{-1}.

These results are explained as follows: for low b there are direct collisions between the two reactants, and it is at the first impact among them when the energy is exchanged. At this moment a proton hop is produced or not, and the energy is transferred to some specific modes. This energy can flow among the different modes, but it is not efficient enough to produce a second proton hop necessary to yield to exchange mechanism. This explains why this last exchange mechanism always occurs with lower probability.

At higher impact parameters the system is rotationally excited, so that, after the first collision, the resulting fragments still keep some time orbiting around each other. This explains why the collision time increases significantly for $b > 10$ a.u. In addition, probably because the appearance of rotational barriers, the identity channel increases, becoming the dominant one. In contrast, the hop and exchange mechanisms probability and the hop/exchange ratio, α, decrease because, after the first proton hop, the system keeps orbiting making a second proton hop more favorable, giving rise to the exchange process in Eq. (1). As energy decreases the maximum impact parameter increases, yielding an increase of the
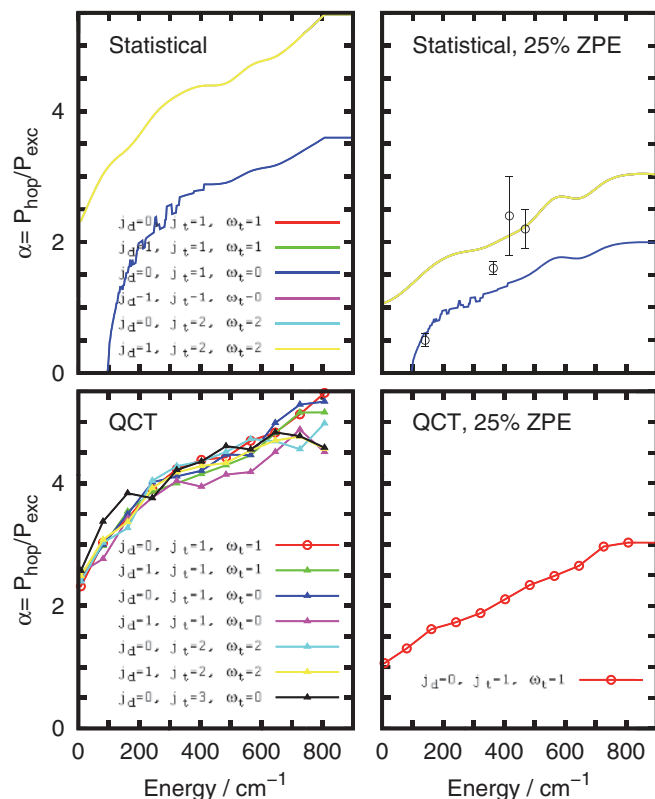
FIG. 5. Hop/exchange ratio, $\alpha(E)$, obtained with different methods. The QCT results are displayed in the bottom panels with the total (left panel) and reduced to 25% (right panel) initial ZPE energies. The top panels are the statistical results including nuclear spin statistics with the $S_{M'}$ matrices obtained from normal (left) and reduced (right) ZPE's QCT calculations. The collision energy is in cm^{-1} and the results are shown for different rotational states of the H$_3^+$(j_t, ω_t) and H$_2$(j_d) fragments. The full PES has been used to calculate the statistical results. In the top-right panel the experimental results of Refs. 13 and 17, measured at 135, 350, 400, and 450 K, plotted at an energy of $\frac{3}{2}k_B T$.

hop/exchange ratio α, as shown in the left-bottom panel of Fig. 5.

D. Scrambling matrix and hop/exchange ratio

The statistical model described above, for the three interaction potential used so far, yield essentially to a constant value of $\alpha(E) = P^{hop}/P^{exchange}$ and equal to 1/2. This factor appears when the degeneracy factor for each rearrangement channel, given by the scrambling matrix, $S_{M'}$, is included in the pure statistical limit described above (1/10, 3/10, and 6/10 for the hop and exchange processes, respectively). When $S_{M'}$ is independent of energy, as in this statistical limit, the $\alpha(E) = P^{hop}/P^{exchange}$ ratio is also constant.

The $\alpha(E)$ ratio may depend on energy if $S_{M'}$ also does, as suggested by Park and Light.[28] It can be considered that $S_{M'}$ is equal to the reaction probabilities on the different rearrangement channels obtained in the QCT calculations and shown in Fig. 3. These probabilities are very similar for all the initial states of the two fragments studied. Thus, to simplify we shall use one common set of results for all of them, in this case those corresponding to the ground levels of reactants. In the statistical limit $S_{M'}$ is the degeneracy of the different rear-

rangement channels. Using the QCT probabilities is a way to introduce a bias due to the dynamics. In particular, the variation of $S_{M'}$ could be attributed to an increasing contribution of a direct mechanism in the reaction, in which the two reactants collide, producing some times a proton hop, with a probability governed also by the dynamics. In this interpretation, the probability of the exchange mechanism can be used to extract the percentage of statistical mechanism versus a direct one.

In order to analyze the effect of using this dynamically biased $S_{M'}(E)$, it is interesting to eliminate first the nuclear spin statistic effect, to be consistent with the QCT calculations. This was done by eliminating the sums over the nuclear spin and the matrices g_{Is} and $\gamma_{sIs'}^{M'}$ in Eqs. (3) and (4). The results obtained for the $\alpha(E)$ ratio are nearly identical for all the initial states considered and very similar to the QCT results, in the bottom-left panel of Fig. 5.

When the nuclear spin statistic is included, the α ratio, in the top-left panel of Fig. 5, keeps essentially the same as for the QCT method. There are some cases, as for $j_d = 0$, $j_t = 1$, $\omega_t = 0$, for which α gets significantly lower. This situation happens when the lower vibrational states corresponding to the hop mechanism are missing by spin statistic while the exchange channel presents open states. In such situations, the hop probability is zero so $\alpha = 0$ as well, even when the exchange probability is different from zero. Thus, when the first levels of the hop channel become open, the α ratio increases but keeps significantly lower than the rest of the cases.

The α ratios obtained are significantly lower than the experimental values of Crabtree *et al.*[17] of 0.5 ± 0.1 at 135 K and 1.6 ± 0.1 at 350 K, and those of Cordonnier *et al.*,[13] being 2.4 ± 0.6 at 400 K. The fact that the experimental value at 135 K is 0.5 may be taken as an indication that the process at this lower temperature is statistical. When the temperature increases this ratio α increases, as it is also the case in the QCT calculations shown here, so that it may be explained accordingly. At low energies, large impact parameters are accessible, corresponding to high orbital angular momentum, giving rise to long-lived resonances. The fragmentation of these long-lived complexes yields a significantly larger exchange probability, according to statistical models. At higher energies, the impact parameter decreases and the two reagents collide more directly, producing a proton hop. The energy redistribution needed for a second hop (to yield an exchange process) is not transferred efficiently probably because the H$_5^+$ complex does not live long enough.

E. Zero-point energy effects

In spite of reproducing the rise of $\alpha(E)$ with increasing collision energy, its simulated value is by far too high as compared to the experimental one. This may be explained as an artifact due to the quasi-classical approximation because of the high ZPE of the fragments, of 6538 cm^{-1}. The H$_5^+$ complex has a ZPE of 7167 cm^{-1}[44] with respect to the minimum of the well, 2415 cm^{-1} below the energy of the ground state of the reactants (see Fig. 6). The ZPE is nearly constant in the entrance channel until the reactants get close enough, where this energy flows to the soft modes of the H$_5^+$ complex, and

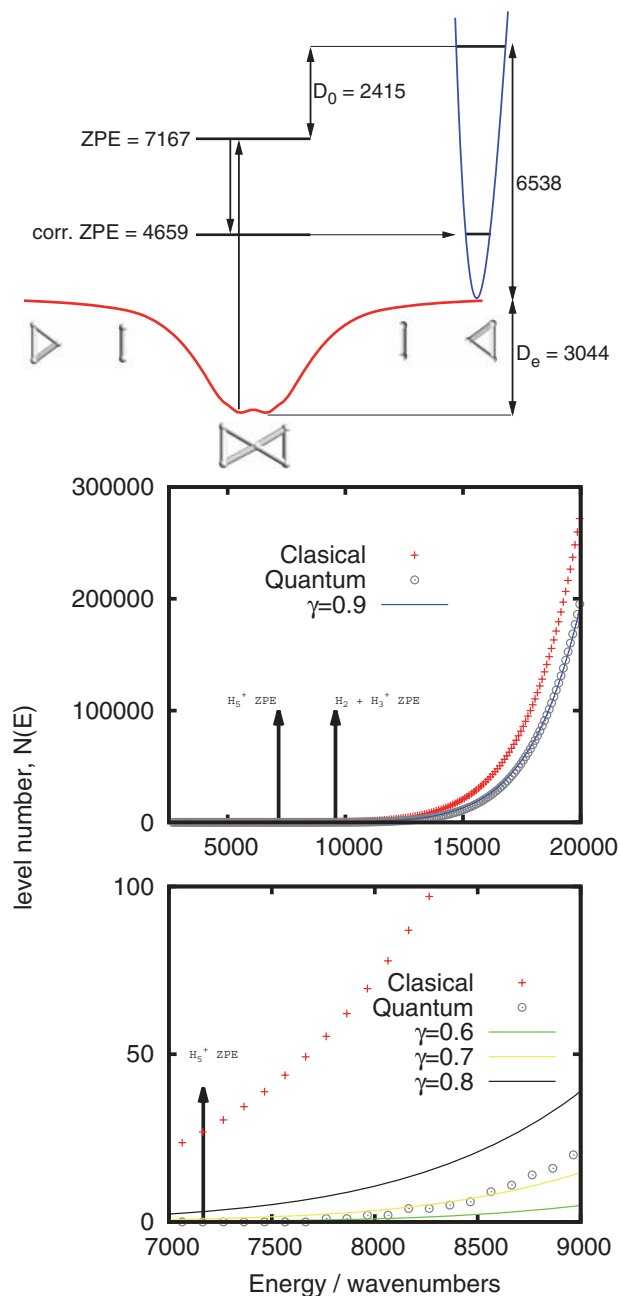FIG. 6. Quantum and classical level numbers obtained for H_5^+ as a function of energy (in cm^{-1}) referred to the bottom of the potential H_5^+ well, as shown in the energy diagram of the top panel. The frequencies of the normal modes used are 4118.15, 3667.19, 2140.31, 1847.43, 1170.36, 866.48, 811.30, 499.76, and 208.09 cm^{-1}. Two different energy regimes are considered in the bottom and middle panels, and the ZPE-corrected level density with the γ factor closer to the quantum results is shown.

the classical nature of the propagation is no longer able to describe the ZPE of H_5^+. This situation leads the system to dispose of an excess of energy which manifests by an unphysical fast dissociation of the complex.

There are many approaches to correct the improper treatment of zero-point energy in classical mechanics.[48–50] One method used in bimolecular reactions are based on reduced dimensionality models, keeping the active modes and correcting the ZPE of the remaining ones in the effective potential.[51] This approach has the inconvenient in H_5^+ that all the atoms

are identical and freezing any mode would introduce artifacts in the probabilities of the different reaction channels. Other methods are classified as "active" or "passive." In the first type, individual trajectories are modified to satisfy the ZPE requirements, as, for example, by preventing the vibrational energy in any mode from falling below its zero-point value.[52] A quite widely used "passive" method consists in reducing the ZPE so that the quantum and classical level numbers coincide as much as possible.[48, 50, 53, 54] This method has been normally applied to unimolecular reactions[48, 53, 54] and can be justified using Rice–Ramsperger–Kassel–Marcus (RRKM) theory by considering that the RRKM unimolecular rate constant is expressed as

$$K(E) = \frac{N(E)}{h\rho(E)}, \qquad (12)$$

where $N(E)$ is the level number at the transition state and $\rho(E)$ is the density of states of products. This expression is valid for quantum and classical mechanics, and in order to obtain the same rate constants, both $N(E)$ and $\rho(E)$ have to be approximately the same for the two theories. This makes necessary to correct the classical quantities, as already demonstrated,[50] by correcting the ZPE, in analogy to what is done in classical trajectory studies.

The level number $N(E)$ has been calculated for the H_5^+ at the minimum of the well using the normal mode frequencies in the quantum and classical approaches. The quantum one is calculated simply counting the number of levels accessible at each energy. The classical one has been calculated with the usual expression[50, 54]

$$N(E) = \frac{E^n}{n! \prod_{i=1}^n \hbar\omega_i}, \qquad (13)$$

where $n = 9$ is the number of normal modes of the system. The corrected $N(E)$ has been calculated as a function of the ZPE reduction, γ, as[50, 54]

$$N(E, \gamma) = N(E - [1 - \gamma]E_{ZPE}). \qquad (14)$$

The γ reduction of the E_{ZPE} is larger in the low energy region of interest in this work, with $\gamma \approx 70\%$–80%, and for larger energies it gets a value of $\gamma \approx 90\%$, as shown in Fig. 6.

In this work we are interested in bimolecular reactions, divided in two steps, the formation and the dissociation of the H_5^+ complex. If all the initial ZPE is used in standard QCT calculations the dissociation of the complex is by far too fast at low collision energies as described above, because the classical level number of H_5^+ is too high. As in unimolecular reaction, the ZPE has to be reduced. Since the critical processes are the formation and destruction of H_5^+, we consider here that the reactants ZPE should be reduced to the value of the modified H_5^+ complex (65% of 7167 cm^{-1}) minus the asymptotic PES ($D_0 = 3044$ cm^{-1}), as illustrated in the top energy diagram of Fig. 6. This quantity would correspond to ≈ 1615 cm^{-1}, about $\approx 25\%$ of the reactants ZPE (6538 cm^{-1}), and would warranty that when the two reactants approach each other at very low collision energy they "find" the corrected density of states of the H_5^+ complex, providing an improvement of the formation/destruction dynamics. Following the arguments described above the correction factor γ

increases when increasing energy. However, in this work we focus on rather low energies and we consider only one reduction value, 25% E_{ZPE}.

The association in ion-molecule collisions has been studied previously using QCT methods.[55–57] While increasing translational energy seems to always reduce the association probability, the effect of ZPE presents more complicated situations. In many cases the inclusion of ZPE in QCT yields to an increase of association probabilities, depending on which modes are included.[56,57] In contrast, the association of H atoms on diamond surface seems to decrease when increasing ZPE of the lattice.[58] This non-clear landscape makes think that the role of the ZPE on the association probability is a complicated energy transfer event, depending on the PES, the masses, well depth, ZPEs, etc.

Since the association probability plays the role of increasing the statistical behavior in $H_2 + H_3^+$ collisions, it is of great interest here to examine the role of ZPE. Here we only consider a reduction of only 25% of the ZPE (1634 cm^{-1}), as discussed above. The collision time and the hop/exchange probabilities versus impact parameters are shown in the right panels of Fig. 4 for different collision energies. The collision times with only 25% of the ZPE are considerably longer than with the full ZPE. In the entrance channel, the process is adiabatic and the collision energy remains constant until the two reactants are close enough to exchange energy. Therefore, the increase of the collision time is essentially due to the formation of complexes with longer lifetimes. Thus, in the present case, the increase of the ZPE inhibits the formation of the complex or association. When the collision energy increases, long impact parameters yield significant shorter collision times, demonstrating that the association probability also decreases with increasing collision energy.

With regards to hop probability (full triangles) it is not affected by the ZPE of reactants: the results obtained with 25% of the ZPE are essentially the same as those obtained with the full ZPE. However, the exchange probability (empty squares) increases significantly, except for the higher collision energy shown, being essentially the same for all impact parameters, except for the longer ones. Consequently, the identity channel decreases when the exchange increases. This demonstrate, that the ZPE introduced in QCT avoids the formation of the complex, since in classical mechanics it flows towards other modes favouring a fast dissociation.

The α ratio obtained with 25% of the ZPE decreases significantly, as shown in the right-bottom panel of Fig. 5, simply because the collision time increases when the available energy decreases. As in the case with 100% of the ZPE, the identity/hop/exchange probabilities obtained are used as $S_{M'}$. This is first tested without spin statistic (lower-right panel) and finally with the spin nuclear statistic and the full PES, as shown in the top-right panel. The behavior is similar to that obtained with the normal QCT probabilities but significantly shifted towards lower values. In this case, when they are compared with the available experimental data[13,17] the agreement is remarkably good, specially for such simple model. The experimental value at 135 K of Crabtree *et al.*[17] is much lower than the one obtained here, and very close to the statistical limit. In order to improve the present results, quantum cal-
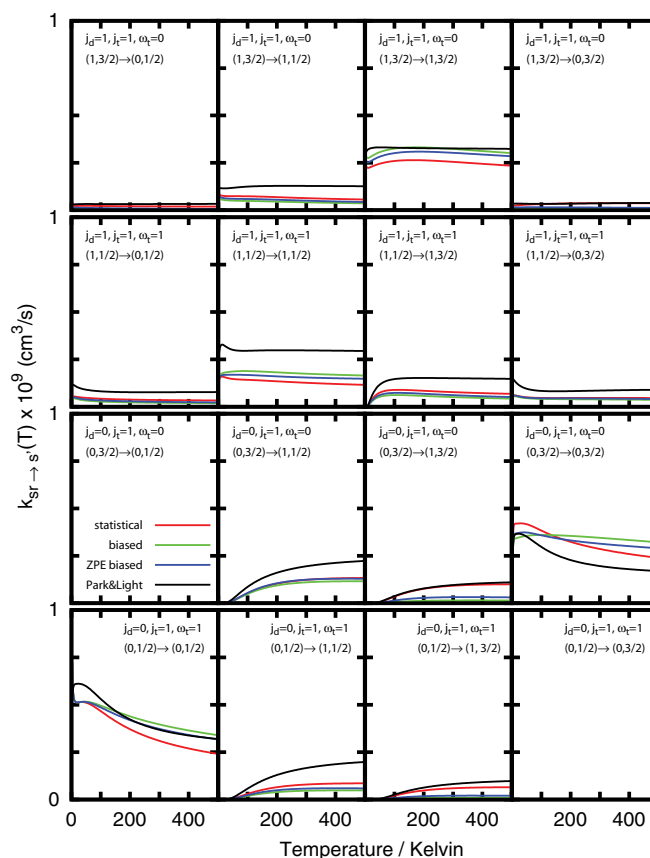

FIG. 7. Reaction rate coefficients obtained by summing of final rotational states, r' and all the 3 mechanisms, using the normal statistical and the two dynamically biased models and the full PES of Ref. 29. Also, the results obtained with the anisotropic asymptotic potential and the pure statistical model, corresponding to that of Ref. 28, are shown.

culations at energies close to the threshold should be done to check to what extent the situation is statistical. The resonances at threshold can be reached by infrared absorption, and the spectrum recorded by detecting the H_3^+ fragments.[59–61] Recently, several quantum approximate and/or reduced dimensionality simulations of the predissociation spectrum have been performed[44,61,62] providing some physical assignment. The agreement between experiment and theory is still quite poor, what demonstrate the need of designing new quantum methods to include all degrees of freedom and the permutation symmetry in this problem.

F. Rate constants

The CRPs have been calculated with the different scrambling matrices, the high temperature statistical limit, the QCT, and ZPE-corrected QCT. These CRPs are integrated in energy, according to Eq. (2), to get the state-to-state rate constants, which are shown in Fig. 7 for the first rotational states of the fragments. The integration in energy in Eq. (2) has been done numerically in the interval $0 < E < 2500$ cm^{-1}. We compare 4 different statistical results. The first ones, corresponding to those reported by Park and Light,[28] are obtained with the asymptotic anisotropic PES and the statistical scrambling matrix $S_{M'}$. The results are essentially the same as those reported previously[28] except in some diagonal terms in which
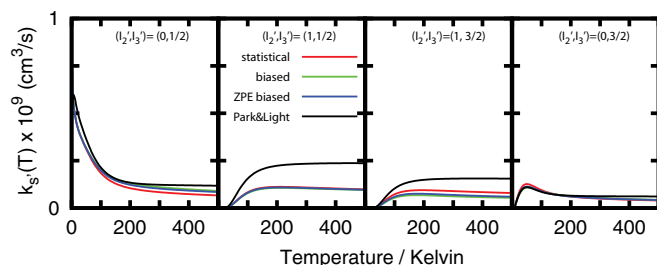
FIG. 8. Same as in Fig. 7 but after average over the initial rotational, r, and spin, s, states of the reactants with a Boltzmann distribution.

there is a small discrepancy attributed to the different methods used here to calculate the capture probability. The second, denoted by statistical, uses the full PES and also the statistical scrambling matrix. These last results are in most of the cases significantly lower than those of Park and Light[28] and the difference can only be attributed to the effect of the anisotropic charge distribution of H_3^+, as commented above for the CRP. The other two cases correspond to the use of the full PES with the two biased scrambling matrices, one obtained from normal QCT calculations and the second with the ZPE-corrected QCT calculations. These two last cases are in general significantly closer to those obtained with the second statistical $S_{M'}$ matrix in which the full PES was used. This shows that the main reason for the difference corresponds to the use of the full PES, while the statistical matrix introduces smaller changes between the two statistical models for these quantities.

In all the cases the trends are rather similar, showing an initial raise or decrease for low temperatures, followed by a plateau for $T > 200$ K. This behavior is typical in ion-molecule collision and explained by simple Langevin models.[11,63] This effect is even more obvious when the average over the initial states of the fragments is performed, as shown in Fig. 8, in which the rotationally thermalized rate constants are essentially constant for $T > 100$ K. In this case, we also observe the influence of incorporating the anisotropy of the charge distribution of H_3^+, being more important than considering a more refined scrambling matrix.

This is not the case when considering the $\alpha(T)$ hop/exchange ratio which is very much dependent on the $S_{M'}$ scrambling matrix, as it is shown in Fig. 9. $S_{M'}$ = 1:3:6 correspond to the number of channels for the identity:hop:exchange mechanisms, independently of temperature and nuclear spin-statistic. When this last effect is accounted for in the statistical model, at low energies some levels disappear, changing the ratio between these mechanisms. That is why, at low temperatures the $\alpha(T)$ ratio shows a minimum at ≈ 20 K. At higher energies, however, these effects disappear because the number of allowed levels for each nuclear spin combination becomes approximately the same, making $\alpha(T)$ = 1/2. Thus, the 1:3:6 ratio becomes the statistical ratio in the high temperature limit.

On the contrary, when using QCT dynamically biased scrambling matrices, this ratio changes a lot. It is important to note that the experimental values available[13,17] change from the statistical value of 1/2 at $T = 125$ K up to a value of ≈ 2
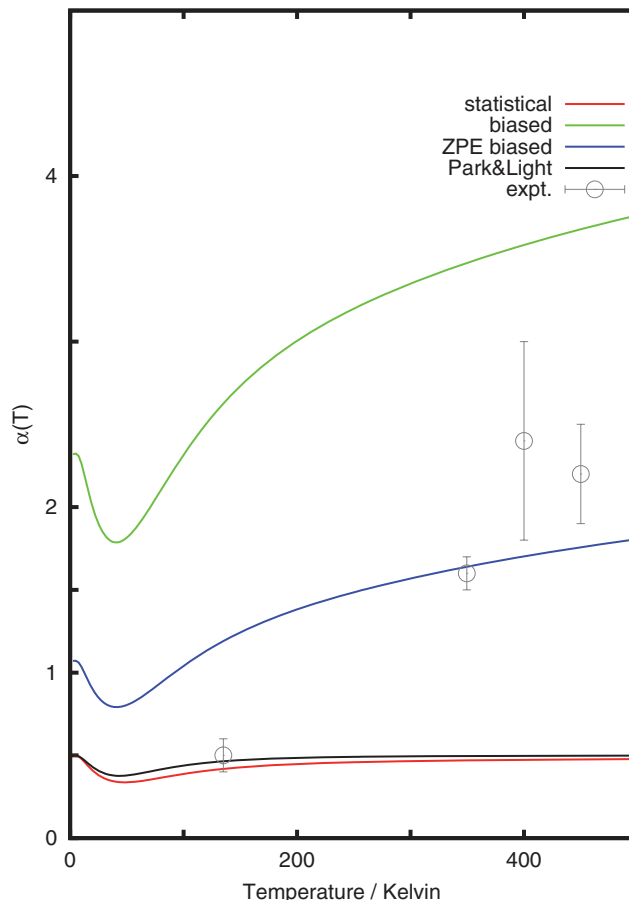

FIG. 9. Thermally averaged $\alpha(T) = K^{hop}/K^{exchange}$ ratio obtained with different versions of the statistical method, as described in the text. The experimental results at 400 K are due to Cordonnier *et al.*,[13] and the rest to Crabtree *et al.*[17] The value at 450 K was described there as preliminary.

for $T > 300$ K. According to the present results, this last value may be explained by an important contribution of direct collisions, producing the hop of a proton, in which the H_5^+ does not live long enough to form a significant amount of exchange reactions.

It is particularly interesting to note that the ZPE-biased scrambling matrix yields results in rather good agreement for the higher temperature measurements, and overall good behavior with the temperature. On the contrary, the QCT biased results are significantly higher. It clearly demonstrates that the reduction of the ZPE has an enormous influence at low temperatures. This was interpreted above by the failure of the QCT approach in considering the ZPE energy along the reaction, and demonstrates that for these low energies it is necessary to incorporate quantum effects, essentially the ZPE. In spite of the simplicity of the model used to account for the ZPE effect, the reasonable agreement with the experimental results available[13,17] already demonstrate its validity. Of course, this description is quite crude and needs to be further validated by quantum methods.

According to the analysis of the classical trajectories made above, at low collision long lived complexes are formed, corresponding to resonances near the dissociation threshold in a quantum description. It is therefore necessary to simulate such processes using quantum methods to treat the

collision including relatively high total angular momenta. This situation complicates the use of iterative procedures, such as the multi-configurational time dependent Hartree method.[64] These resonances close to the dissociation threshold are accessible by infrared excitation from the H_5^+, and there are several experimental results on this system and its isotopic variants.[59–61,65] If the hypothesis discussed above is true, there may be some differences in the broadening of the resonances near the dissociation threshold as a function of the total angular momentum excitation, and this could be probably measured by changing the experimental rotational temperature of the experiments. Also, there have been several theoretical simulations on this infrared predissociation spectra,[44,61,62] but they use either approximate methods or reduced dimensionality models which need to be improved to account for the narrow resonances at high J with enough accuracy to extract information relevant for the transition between statistical and direct regimes in the collisions discussed in this work.

III. CONCLUSIONS

This work presents a combined statistical/classical trajectory study of the $H_3^+ + H_2$ collisions, which supposes an extension of a previous statistical method by Park and Light.[28] Two new ingredients are considered in the present treatment; first, we use the full multidimensional PES to account for the anisotropy of the H_3^+ fragment and the H_5^+ well depth, and second, we use QCT calculations to generate a scrambling matrix which depends on the collision energy, as already proposed by Park and Light.[28] This new matrix accounts for the transition between full scrambling statistical mechanism, at low energies (below 50 cm^{-1}) and direct hop mechanisms at higher energies, allowing a reasonable description of the $\alpha(T) = K^{hop}/K^{exchange}$ ratio determined experimentally.[13,17] The rate constants obtained in the $0 < T < 500$ K interval are slightly lower than the previously obtained ones,[28] simply because the anisotropy and the shallow well of the full PES reduce the probability of forming the H_5^+ complex.

It is found that the ZPE plays a key role in the dynamics.[11] The use of the ZPE of the fragments in QCT calculations leads to wrong results because this energy redistributes, reducing the lifetime of the H_5^+ complexes. This makes that the full scrambling is not longer probable enough to obtain a good $\alpha(T) = K^{hop}/K^{exchange}$. Reducing the ZPE of the reactants yields to a considerably improved scrambling matrix, and the α ratios obtained are in better agreement with experimental results. This reduction of the ZPE is explained by the need of correcting the pure classical level number of the H_5^+ complex, as done in classical simulations of unimolecular processes and to get equivalent quantum and classical rate constants using RRKM theory. At the time being and due to the complexity of the H_5^+ system, this reduction of the ZPE cannot be further validated either with the exact theory nor on another smaller system. Future studies have to be done in that direction.

The analysis of the QCT calculations indicates that trajectories responsible for the longer lived dynamics and the higher exchange proportion are those occurring at large impact parameters at very low collision energy, below 50 cm^{-1}. This indicates that to improve the dynamical description made here it is necessary to use quantum methods describing relatively high total angular momenta and low kinetic energy. Such studies are now-a-days a challenge and some approximations are in progress. It is well known that in hydrogen plasmas at room temperature the title reaction, and isotopologues, do not play a significant role in the proportion of the deuterated H_3^+.[8,9] However, at the lower temperatures of the interstellar medium, $\approx$10 K, these collisions are thought to be one of the most important ones in explaining the anomalous high proportion of deuterated triatomic hydrogen ions,[7] giving rise to the deuteration of other molecular species in space.

[1]T. J. Millar, A. Bernett, and E. Herbst, Astrophys. J. **340**, 906 (1989).
[2]L. Pagani, M. Salez, and P. Wannier, Astron. Astrophys. **258**, 479 (1992).
[3]J. Tennyson, Rep. Prog. Phys. **58**, 412 (1995).
[4]B. J. McCall and T. Oka, Science **287**, 1941 (2000).
[5]L. E. Moore, M. Mendillo, I. Müller-Wodarg, and D. L. Murr, Icarus **172**, 503 (2004).
[6]O. Witasse, T. Cravens, M. Mendillo, J. M. A. Kliore, A. Nagy, and T. Breusx, Space Sci. Rev. **139**, 235 (2008).
[7]D. L. Huestis, S. W. Bougher, J. L. Fox, M. Galand, R. E. Johnson, J. I. Moses, and J. C. Pickering, Space Sci. Rev. **139**, 63 (2008).
[8]I. Méndez, F. J. Gordillo-Vázquez, V. J. Herrero, and I. Tanarro, J. Phys. Chem. A **110**, 6060 (2006).
[9]M. Jiménez-Redondo, E. Carrasco, V. J. Herrero, and I. Tanarro, Phys. Chem. Chem. Phys. **13**, 9655 (2011).
[10]D. S. N. G. Adams and E. Alge, Astrophys. J. **263**, 123 (1982).
[11]K. Giles, N. G. Adams, and D. Smith, J. Phys. Chem. **96**, 7645 (1992).
[12]D. Uy, M. Cordonnier, and T. Oka, Phys. Rev. Lett. **78**, 3844 (1997).
[13]M. Cordonnier, D. Uy, R. M. Dickson, K. Kerr, Y. Zhang, and T. Oka, J. Chem. Phys. **113**, 3181 (2000).
[14]D. Gelich and S. Schlemmer, Planet. Space Sci. **50**, 1287 (2002).
[15]D. Gerlich, E. Herbst, and E. Roueff, Planet. Space Sci. **50**, 1275 (2002).
[16]E. Hugo, O. Asvany, and S. Schlemmer, J. Chem. Phys. **130**, 164302 (2009).
[17]K. N. Crabtree, C. A. Kauffman, B. A. Tom, E. Becka, B. A. McGuire, and B. J. McCall, J. Chem. Phys. **134**, 194311 (2011).
[18]T. J. Millar, Planet. Space Sci. **50**, 1189 (2002).
[19]L. Pagani, C. Vastel, E. Hugo, V. Kokoouline, C. H. Greene, A. Bacmann, E. Bayer, C. Ceccarelli, R. Peng, and S. Schlemmer, Astron. Astrophys. **494**, 623 (2009).
[20]T. A. Bell, K. Willacy, T. G. Phillips, M. Allen, and D. Lis, Astrophys. J. **731**, 48 (2011).

[21]F. Fontani, A. Palau, P. Caselli, A. Sánchez-Monge, M. J. Butler, J. C. Tan, I. Jimémez-Serra, G. Busquet, S. Leurini, and M. Audard, Aston. Astrophys. **529**, L7 (2011).

[22]D. Gerlich, J. Chem. Phys. **92**, 1141 (1990).

[23]M. Quack, Mol. Phys. **34**, 21 (1977).

[24]T. Oka, J. Mol. Spectrosc. **228**, 635 (2004).

[25]D. Gerlich, F. Windisch, P. Hlavenka, R. Plasil, and J. Glosik, Philos. Trans. R. Soc. London, Ser. A **364**, 3007 (2006).

[26]K. Park and J. C. Light, J. Chem. Phys. **127**, 224101 (2007).

[27]K. N. Crabtree, B. A. Tom, and B. J. McCall, J. Chem. Phys. **134**, 194310 (2011).

[28]K. Park and J. C. Light, J. Chem. Phys. **126**, 044305 (2007).

[29]A. Aguado, P. Barragan, R. Prosmiti, G. Delgado-Barrio, P. Villarreal, and O. Roncero, J. Chem. Phys. **133**, 024306 (2010), see http://fama.iff.csic.es/personas/octavio/metodos-programas/PES/PES.html.

[30]P. Barragan, R. Prosmiti, O. Roncero, A. Aguado, P. Villarreal, and G. Delgado-Barrio, J. Chem. Phys. **133**, 054303 (2010).

[31]U. Nagashima, K. Morokuma, and H. Tanaka, J. Phys. Chem. **96**, 4294 (1992).

[32]W. Kraemer, V. Spirko, and O. Bludský, J. Mol. Spectrosc. **164**, 500 (1994).

[33]R. Prosmiti, A. A. Buchachenko, P. Villarreal, and G. Delgado-Barrio, Theor. Chem. Acc. **106**, 426 (2001).

[34]G. E. Moyano and M. A. Collins, J. Chem. Phys. **119**, 5510 (2003).

[35]Z. Xie, B. J. Braams, and J. M. Bowman, J. Chem. Phys. **122**, 224307 (2005).

[36]A. Kuppermann, J. Phys. Chem. **113**, 4518 (2009).

[37]A. Kuppermann, private communication (2010).

[38]A. Kuppermann, Phys. Chem. Chem. Phys. **13**, 8259 (2011).

[39]D. Wang, Z. Xie, and J. M. Bowman, J. Chem. Phys. **132**, 084305 (2010).

[40]A. Aguado, O. Roncero, C. Tablero, C. Sanz, and M. Paniagua, J. Chem. Phys. **112**, 1240 (2000).

[41]A. Aguado, M. Lara, M. Paniagua, and O. Roncero, J. Chem. Phys. **114**, 3440 (2001).

[42]R. Zare, *Angular Momentum* (Wiley, 1988).

[43]M. Karplus, R. N. Porter, and R. D. Sharma, J. Chem. Phys. **43**, 3259 (1965).

[44]A. Aguado, C. Sanz-Sanz, P. Villarreal, and O. Roncero, Phys. Rev. A **85**, 032514 (2012).

[45]L. Bonnet and J.-C. Rayez, Chem. Phys. Lett. **277**, 183 (1997).

[46]L. Bonnet and J.-C. Rayez, Chem. Phys. Lett. **397**, 106 (2004).

[47]P. G. Jambrina, J. M. Alvariño, D. Gerlich, M. Hankel, V. J. Herrero, V. Sáez-Rábanos, and F. J. Aoiz, Phys. Chem. Chem. Phys. **14**, 3346 (2012).

[48]D.-h. Lu and W. L. Hase, J. Chem. Phys. **91**, 7490 (1989).

[49]Y. Guo, D. L. Thompson, and T. D. Sewell, J. Chem. Phys. **104**, 576 (1996).

[50]G. Stock and U. Müller, J. Chem. Phys. **111**, 65 (1999).

[51]J. M. Bowman, A. F. Wagner, S. Walch, and T. H. Duning, J. Chem. Phys. **81**, 1739 (1984).

[52]W. M. Miller, W. L. Hase, and C. L. Darling, J. Chem. Phys. **91**, 2863 (1989).

[53]T. Uzer, B. D. MacDonald, Y. Guan, and D. L. Thompson, Chem. Phys. Lett. **152**, 405 (1988).

[54]P. Manikandan and W. L. Hase, J. Chem. Phys. **136**, 184110 (2012).

[55]J. V. Dugan and R. B. Canright, J. Chem. Phys. **56**, 3623 (1972).

[56]W. L. Hase, C. L. Darling, and L. Zhu, J. Chem. Phys. **96**, 8295 (1992).

[57]W. L. Hase and Y. J. Cho, J. Chem. Phys. **98**, 8626 (1993).

[58]C. Accary, P. Barbarat, W. L. Hase, and K. C. Hass, J. Phys. Chem. **97**, 9934 (1993).

[59]M. Okumura, L. Yeh, and Y. Lee, J. Chem. Phys. **83**, 3706 (1985).

[60]M. Okumura, L. Yeh, and Y. Lee, J. Chem. Phys. **88**, 79 (1988).

[61]T. C. Cheng, B. Bandyopadyay, Y. Wang, S. Carter, B. J. Braams, J. M. Bowman, and M. A. Duncan, J. Phys. Chem. Lett. **1**, 758 (2010).

[62]C. Sanz-Sanz, O. Roncero, A. Valdes, R. Prosmiti, G. Delgado-Barrio, P. Villarreal, P. Barragan, and A. Aguado, Phys. Rev. A **84**, 060502(R) (2011).

[63]S. C. Smith and J. Troe, J. Chem. Phys. **97**, 5451 (1992).

[64]M. H. Beck, A. Jäckle, G. A. Worth, and H.-D. Meyer, Phys. Rep. **324**, 1 (2000).

[65]Y. K. Bae, Chem. Phys. Lett. **180**, 179 (1991).